

BEHAVIOR OF PRECAST CES COLUMNS FOR MIDDLE AND LOW-RISE HOUSES

Takanori Kawamoto¹, Hiroshi Kuramoto², Tomoya Matsui³, Toshiaki Fujimoto⁴ and Junji Osaki⁵

¹ Ube-Mitsubishi Cement Research Institute Corporation, Ube, Japan

² Professor, Dept. of Architectural Engineering, Osaka University, Osaka, Japan

³ Professor, Dept. of Architectural and Civil Engineering, Toyohashi University, Toyohashi, Japan

⁴ Technical Research Center, Ando Corporation, Fujimino, Japan

⁵ Ube-house Corporation, Yamaguchi, Japan

Email: kawamoto@ube-ind.co.jp

ABSTRACT :

Concrete Encased Steel (CES) structural system consisting of only fiber reinforced concrete (FRC) and encased steels only have been proposed by the authors as a new composite structural system, which is being investigated continuously with comprehensive studies to make it practical. A study on precast CES columns was carried out as a part of these studies. The purposes of this study are to investigate the seismic performance of precast CES columns for middle and low-rise houses and to obtain the fundamental data to construct the analytical models of the columns that applicable to pushover analysis to be used in the Calculation of Response and Limit Strength (CRLS), which is a new structural calculation method for buildings introduced in June 2000 by revising the Building Standard Law of Japan.

The precast CES columns are constructed by connecting precast CES elements using high strength bolts and fiber reinforced mortar which is cast into the joint. The precast elements are manufactured by casting FRC over built-in steels. A total of three precast CES columns of about a half scale to the real structure were tested under constant axial load and lateral load reversals that simulated seismic loading. The variables investigated were the connection details between the elements and the compressive strength of FRC used for the precast elements.

This paper outlines the structural testing and discusses the structural performance of the precast CES columns. The results shows that the flexural strength of the columns is developed by the yielding of the encased steel and the lateral deformation capacity reaches a maximum story drift angle, R of 0.05 radian. Moreover, the spalling of cover concrete does not occur even at the story drift angle of 0.05 radian because the FRC works effectively. It is also indicated that the ultimate flexural strength of the CES columns can be calculated by using the AIJ design formulas for SRC members and the shear versus lateral displacement response can be simulated by using the Takeda model.

KEYWORDS: Composite structures, Precast CES column, Fiber reinforced concrete, Experimental testing, Seismic performance

1. INTRODUCTION

Steel reinforced concrete (SRC) structures are typical composite structural system consisting of steel and reinforced concrete (RC), which have excellent earthquake resistance with high capacities and deformability. However, the design process and construction work are more complicated than those for RC structures and steel structures. In order to solve these problems, concrete encased steel (CES) structures have been proposed by the authors (Adachi et al., 2002 and Taguchi et al., 2006), and are being investigated continuously with comprehensive studies to make it practical. In the existing experimental studies on CES columns for high-rise buildings, it was found that the hysteretic characteristics of the CES columns were almost the same as those of SRC columns. However, experimental studies on CES structural system for middle and low-rise houses have not been carried out. In middle and low-rise houses, it is possible to assemble precast CES columns with a small section enabling to reduce the construction time and cost. Moreover, Calculation of Response and Limit

length of 30mm, while the fiber used for the fiber reinforcement mortar filling in the joint part was vinylon fiber (RF400) with the diameter of 0.2mm and length of 12mm. For both types of fiber, the volume mixing ratio in the concrete mixture was 1.5%.

Table 1 The proportions of FRC

Specimen	W/C (%)	Volume mixing ratio of fiber (%)	Unit weight (kg/m ³)					
			Water	Cement	Lime powder	Sand	Gravel	Fiber
FRC-CES PCa-CES1	50	1.5	175	350	100	1129	525	19.5
PCa-CES2	60	1.5	182	300	197	1051	525	19.5

Table 2 Steel properties

Steel	$E_s(N/mm^2)$	$\sigma_y(N/mm^2)$
Flange	2.01×10^5	312
Web	2.01×10^5	318

E_s : Elastic modulus
 σ_y : Yield stress

Table 3 Concrete and mortar properties

Specimen	Compressive strength; $\sigma_B (N/mm^2)$	
	FRC	FRM
FRC-CES	52.9	—
PCa-CES1	51.6	43.0
PCa-CES2	44.3	47.9

2.3. Test setup and loading procedures

The loading apparatus used is shown in Fig.3. The specimen was fixed by PC bars to the reaction frame. The specimen was loaded lateral cyclic shear forces by a horizontal actuator and a constant axial compression of 230kN as a long time loading by a vertical jack. The applied axial force ratio, $N/(bD\sigma_B)$, for the specimen was about 0.1. The incremental loading cycles were controlled by story drift angles, R , which was given by the ratio of lateral displacements to the column height, δ/h . In this experiment, the specimens were cyclically loaded twice for R of 0.0025, 0.005, 0.001, 0.015, 0.02 and 0.03 radians, and once for that of 0.04 and 0.05 radians, respectively.

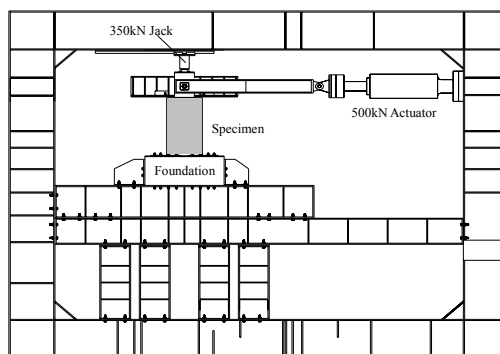


Figure 3 Loading apparatus

3. TEST RESULTS AND DISCUSSIONS

3.1. Failure pattern

Failure patterns of the specimens at R of 0.01 and 0.05 radians are shown in Figure 4. and Photo 1. The development of crack and progress of failure for the specimens are described below.

In the specimen FRC-CES, flexural cracks occurred in the lower part and the center part of the column from R of 0.0025 until R of 0.005 radians. Then the flexural-shear cracks occurred in the center part of the column. After the flexural cracks and flexural-shear cracks extended at R of 0.01 radian, the width of flexural cracks in the lower part of the column extended at R of 0.015 radian. Although the cracks propagated, spalling of cover concrete didn't occur until the maximum story drift, R of 0.05 radian.

In the specimen PCa-CES1, flexural cracks occurred in the lower joint part, the center part and the center joint part of the column from R of 0.0025 until R of 0.005 radian. Although flexural cracks in the lower joint part of the column extended, significant damage was not observed in the center part of the column until R of 0.05 radian. Compared with the specimen FRC-CES, the specimen PCa-CES1 had the less damage, where the damage in the precast columns reduced because the damage concentrated only in the joint part.

In the specimen PCa-CES2, flexural cracks occurred in the center joint part and the lower joint part of the column and diagonal cracks occurred in the bottom of the column from R of 0.0025 to R of 0.01 radians. After the flexural cracks appeared in the lower joint part of the column at R of 0.005 radian, vertical cracks occurred in the cover concrete at the lower part of the compression area of the column. Although compression cracks extended in the cover concrete, significantly destruction was not observed until the maximum story drift, R of 0.05 radian.

Compared with the specimen PCa-CES1 in which the compressive strength of FRC in the precast column was higher than that of PCa-CES2 and the same axial compression was applied. Specimen PCa-CES2 showed a compression failure that occurred in the precast column. This indicates that the compressive strength of FRC affects the failure pattern of the column.

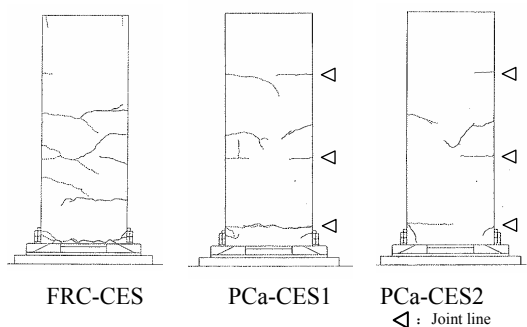


Figure 4 Failure pattern(R of 0.01 rad.)

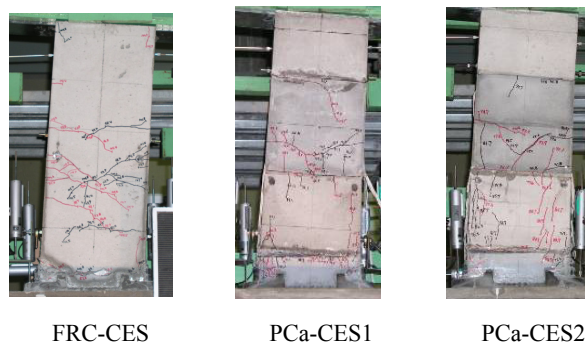


Photo 1 Failure pattern(R of 0.05rad.)

3.2. Hysteresis characteristics

Shear versus story drift angle relationships of the specimens are shown in Fig.5. The yield and maximum strengths and corresponding story drift angles for each specimen are listed in Table 4. The yielding of each specimen was assumed when the first yielding of steel flange at the bottom of the columns was observed, which corresponds to a circle mark on the shear versus story drift angle response (see Fig.5). The calculated flexural strength was indicated on Fig.5 by a dotted line.

All specimens showed ductile and stable spindle-shape hysteresis loops without significant capacity reduction until the maximum story drift, R of 0.05 radian.

In the specimen FRC-CES, the initial stiffness reduced due to the flexural cracks at R of 0.0025 radian. The yielding of steel flange was observed at shear forces of 108.1kN at R of 0.01 radian. Then the maximum strength of 114.5kN was reached at R of 0.03 radian. On the other hand, the significant capacity reduction was not observed until R of 0.05 radian.

Table 4 Measured strength

Specimen		at Yielding		at the Max. Capacity	
		Ry(rad.)	Qy(kN)	Ru(rad.)	Qu(kN)
FRC-CES	+	0.0096	108.1	0.0284	114.5
	-	-0.0087	-105.2	-0.0195	-115.7
PCa-CES1	+	0.0087	99.3	0.0195	103.6
	-	-0.0088	-97.1	-0.0300	-102.9
PCa-CES2	+	0.0089	96.9	0.0149	99.8
	-	-0.0090	-93.9	0.0256	-98.1

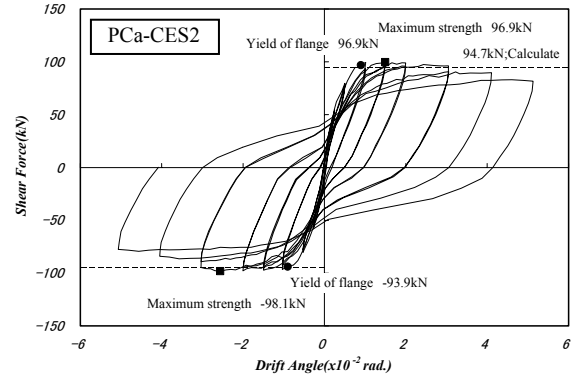
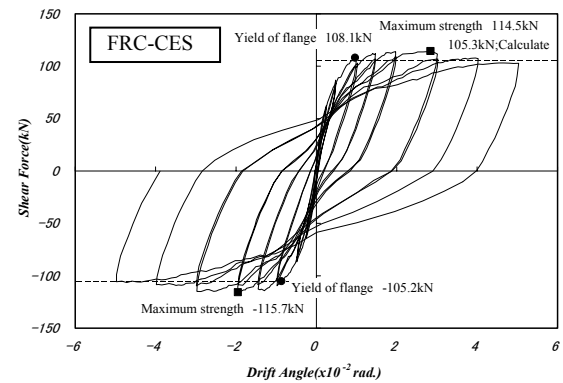
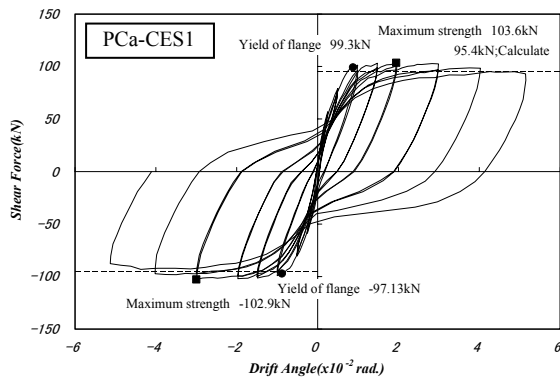


Figure 5 Shear force-story drift angle relationships

In the specimen PCa-CES1 and PCa-CES2, the initial stiffness reduced due to the flexural cracks at R of 0.0025 radian. The yielding of steel flange was observed at R of 0.01 radian. Then the maximum strength was reached at R of 0.02 radian. The significant capacity reduction was not observed until R of 0.05 radian in the specimen PCa-CES1, while the capacity reduction was slightly observed in the specimen PCa-CES2 at R of 0.04 radian due to the compression failure.

Compared with the specimen FRC-CES, the hysteresis curves of the specimens PCa-CES1 and PCa-CES2 showed slightly a slipped type. This indicates that the midheight joint of the precast columns affects the hysteresis loops. On the other hand, the yielding of anchor bolts in the bottom of the specimens was not observed. The hysteresis loops showed ductile and stable spindle-shape mainly because the yielding of steel flange occurred before the yielding of the anchor bolts.

The comparisons between the measured and the predicted flexural strength of the three specimens are also shown in Fig.5. The measured maximum flexural strength of the three specimens fairly agreed with the flexural strength calculated by the existing equations of SRC columns (AIJ, 1987).

4. SIMULATION OF THE SHEAR VERSUS LATERAL DISPLACEMENT RESPONSE

4.1. Simulated program

The non linear analysis using Takeda model was carried out to construct analytical models of the CES column member and elements that applicable to pushover analysis used in CRLS. Figure 6 shows the skeleton curve with illustration of cyclic deterioration in strength and stiffness. The skeleton curve is the Tri-linear curve with Qcr and Qy. Qcr is the flexural cracking strength calculated by the existing equations of RC elements (AIJ,

1999) and Q_y is the flexural strength calculated by the existing equations of SRC columns (AIJ, 1987). The initial stiffness (K_e) is elastic stiffness with flexural deformation, shear deformation and rotation deformation. Then α_y used in the calculated deformation of Q_y is adopted as 0.35, which is developed from test results. In addition, the stiffness after the yielding of steel flange is 1/1000 of K_e and γ is adopted as 0.40, which is also developed from test results.

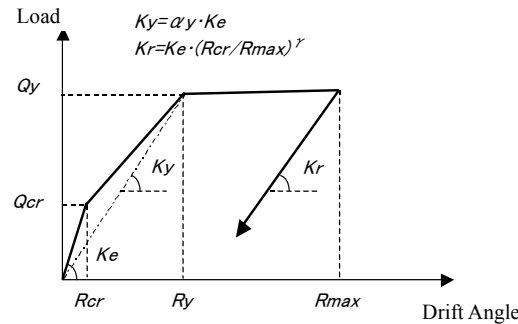


Figure 6 Analytical model

The comparisons between the measured stiffness ratio and the stiffness ratio calculated by $\gamma=0.4$ are shown in Fig.7. In the both specimens, the measured stiffness ratio fairly agreed with the calculated stiffness ratio. It is indicated that the K_r is presented by $\gamma=0.4$.

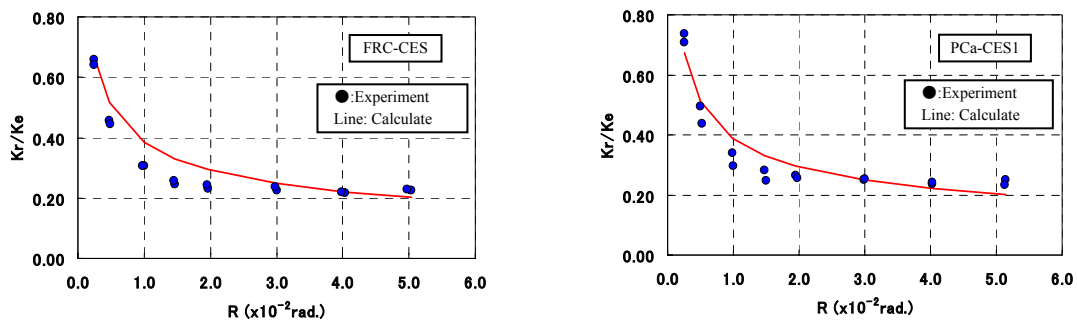


Figure 7 Stiffness ratio (K_r/K_e)

4.2. Simulated result

The comparison of initial stiffness is shown in Table 5. The shear versus story drift angle relationships of the three specimens are compared in Fig. 8. In the figure, the solid lines represent the simulated results and the dotted lines represent the measured hysteresis loops. In the three specimens, the measured initial stiffness agreed with the calculated initial stiffness. In addition, the measured hysteresis curves agreed with the calculated hysteresis curves. This indicates that the hysteresis curves of the FRC-CES and PCa-CES columns can be simulated by using the Takeda model.

Table 5 Initial stiffness (K_e)

Specimen	eKe $\times 10^4 \text{kN/rad.}$	cKe $\times 10^4 \text{kN/rad.}$	eKe/cKe
FRC-CES	4.32	4.06	1.06
PCa-CES1	3.67	3.61	1.02
PCa-CES2	3.27	3.51	0.93

eKe: the measured initial stiffness
 cKe: the calculated initial stiffness

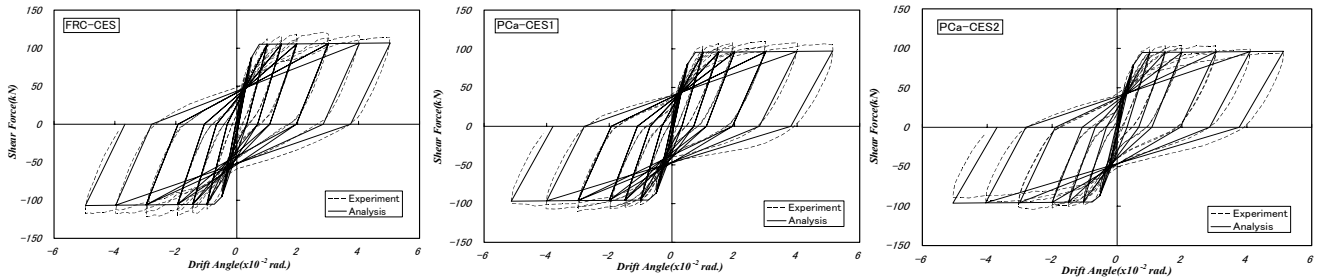


Figure 8 Simulated result

4.3. Accumulated energy and Equivalent viscous damping factor

The comparisons of the accumulated energy and equivalent viscous damping factor of the specimens FRC-CES and PCa-CES1 are shown in Fig.9 and Fig.10, respectively. In the both specimens, the measured accumulated energy fairly agreed with the accumulated energy calculated by using the Takeda model. Also, the measured equivalent viscous damping factors in the second cycle fairly agreed with those of calculated by using the Takeda model. This implies that the equivalent viscous damping factor of the precast CES columns also can be simulated by using the Takeda model.

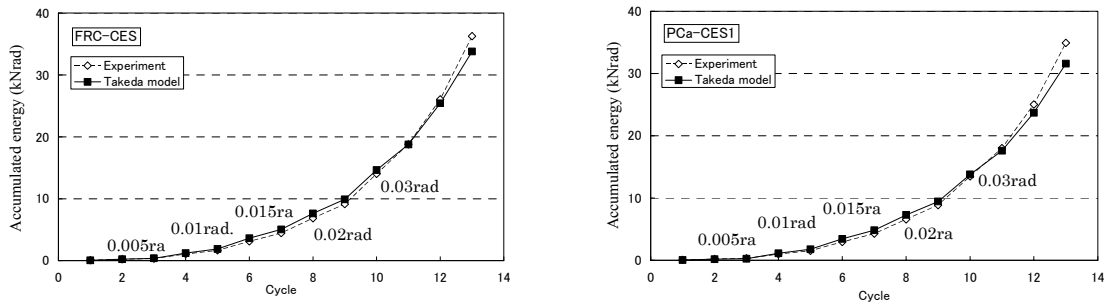


Figure 9 Accumulated energy

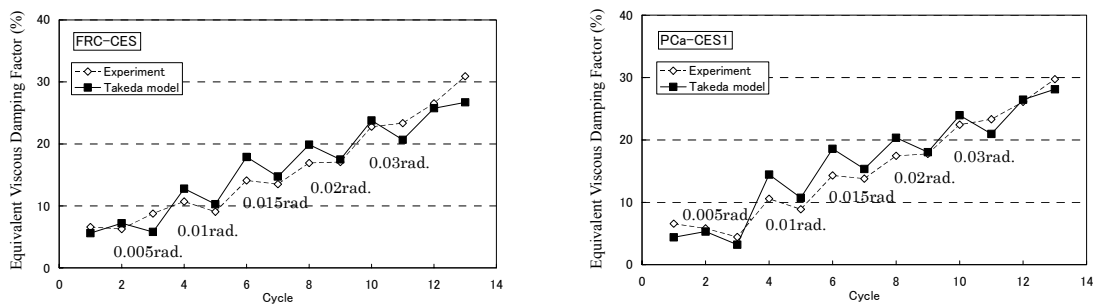


Figure 10 Equivalent viscous damping factor

5. CONCLUSION

An experimental study on precast CES columns for middle and low-rise houses is presented. The conclusions obtained are summarized as follows.

- (1) The deformation capacity of the precast CES columns is about R of 0.05 radian as well as the CES columns.
- (2) Spalling of cover concrete can be prevented until large story drift angle, R of 0.05 radian, by using the FRC.
- (3) The flexural strength of the precast CES columns can be calculated by using the AIJ design formulas for SRC members.
- (4) The shear versus lateral displacement response of the precast CES columns can be simulated by using the Takeda model using parameters $\alpha\gamma=0.35$ and $\gamma=0.4$.
- (5) The equivalent viscous damping factor of the precast CES columns also can be simulated by using the Takeda model.

REFERENCES

- Adachi, T., Kuramoto, H. and Kawasaki, K. (2002). Experimental Study on Structural Performance of Composite Columns Using FRC. *Proceeding of the Japan Concrete Institute* **vol.24, No.2**, 271-276
- Taguchi, T., Nagata, S., Matsui, T. and Kuramoto, H. (2006). Structural Performance of CES Columns encased H-section steel. *Proceeding of the Japan Concrete Institute* **vol.28, No.2**, 1273-1278
- Takeda, T., M.A. Sozen & N.N. Nelson. (1970). Reinforced Concrete response to simulated earthquakes. *Journal of structural division ASCE*, **Vol.96, No.STc2**, 2557-2573
- AIJ. (1987). Standard for Structural Calculation of Steel Reinforced Concrete Structures
- AIJ. (1999). Standard for Structural Calculation of Reinforced Concrete Structures